Electrochemical performance and stability of $Ni_{1-x}Co_x$-based cermet anode for direct methane-fuelled solid oxide fuel cells

Wongsawatgul Nicharee[1], Soamwadee Chaianansutcharit[2] and Kazunori Sato[3,a]

[1] *Program of Petrochemistry, Chulalongkorn University, Thailand & Program of Materials Science, Nagaoka University of Technology, Japan*
[2] *Department of Chemistry, Faculty of Science, Chulalongkorn University, Bangkok, Thailand*
[3] *Department of Materials Science and Technology, Nagaoka University of Technology, Nagaoka, Niigata, Japan*

Abstract. Carbon deposition on Ni-based anode is well-known as a major barrier for the practical use and commercialization of hydrocarbon-fuelled solid oxide fuel cells (SOFCs). In this work, Co alloying in Ni-YSZ was studied as an alternative anode material for using CH_4 as a fuel. The Ni-YSZ and Ni-Co alloyed-YSZ were prepared by the traditional impregnation method without further mixing processes. After sintering and reduction in H_2 atmosphere, the introduced Co can completely dissolved into the Ni lattice and changed the morphology with an increase in the Ni-YSZ grain size and showed a better uniform microstructure. The Co alloying also enhanced the electrochemical performance under CH_4 fuel by reducing the resistance and anodic overvoltage. Moreover, the Co addition enhanced the stability of the cell with CH_4 a constant load current of 80 mA for 60 h. This performance related to the carbon deposition on the anode surface. The Co alloying showed a high efficiency to suppress the carbon deposition and improved the electrochemical performance of an SOFC cell operating under CH_4 fuel.

1 Introduction

Solid oxide fuel cells (SOFCs) are one of the most effective devices to convert chemical energy to electricity. With its high operating temperature (normally >600 °C), SOFCs can run with both hydrogen and hydrocarbon fuels, such as natural gas and ethanol. However, unsolved problems of hydrogen storage have driven a lot of researches on alternative fuels for SOFCs [1-6]. Methane (CH_4) is the simplest hydrocarbon, which is one of the most interested alternative fuels for SOFCs due to its high hydrogen-to-carbon molar ratio and it has a small amount of N and S impurities. Moreover, it is not only the main component of gas and coal-bed gas but also the biogas [7-10]. CH_4 can be therefore considered as a renewable energy.

Ni-YSZ cermet has been known as an effective anode for SOFCs due to its high electrochemical catalytic activity for hydrogen. However, Ni-YSZ cermet showed a coarsening of Ni grains at high temperatures and carbon deposition when hydrocarbons are directly used as fuels. Carbon is easy to form and deposit on a Ni-YSZ anode due to a high catalytic activity of C-H bond braking in hydrocarbons, resulting in reduce fuel utilization but also deactivation of the anode [11]. An addition of water vapor to hydrocarbon fuels is an effective way to moderate the carbon deposition problem [12]. Unfortunately, high H_2O content will deactivate the cell and the system will be more complexed [13]. The replacement of Ni with electronic conductors is another way to avoid the carbon deposition. Cu was reported to avoid the coke formation in methane [14, 15]. However, the diffusion of Cu into YSZ electrolyte results in a YSZ degradation, and the low sintered temperature of Cu limits the operation temperature and decrease catalytic activity for methane conversion [16-18]. With a similar character to Ni, Co has been interested to dope in Ni anode [19]. Co alloying showed a retardation of Ni particle coarsening and enhanced the cell performance in H_2 [20]. Catalytic activity and stability of Ni-Co alloying was enhanced as compared to that of Ni in H_2 containing CO or H_2S as a fuel [21]. Co alloying also reduced the anodic polarization resistance and the amount of carbon deposition on Ni-GDC under a CH_4 fuel [22].

However, the precise mechanism of preventing carbon deposition by Co-alloying to Ni in the cermet anode is still unclear and the electrochemical performance stability has not been carefully studied. In this research, we have investigated the influence of Co alloying in conventional Ni/YSZ cermet in term of morphology and the electrochemical performance, especially the stability of the cell in dry methane.

2 Experimental

The $Ni_{1-x}Co_xO$-YSZ cermet (x=0 and 0.15) was prepared by the traditional impregnation method. This process was started with on appropriate amount of $Ni(NO_3)_2 \cdot 6H_2O$ (98% purity, Nacalai Tesque) and $Co(NO_3)_3 \cdot 9H_2O$ (98%

[a] Corresponding author: sato@analysis.nagaokaut.ac.jp

purity, Nacalai Tesque) were dissolved in distillated water, and then YSZ (8mol% Y_2O_3-ZrO_2, 99.9% purity, Tosoh Corp.) powder was proportionately added into the solution with the composition of 60%$Ni_{1-x}Co_xO$ + 40%YSZ (wt.%). After dehydration, the obtained powder was calcined at 800 °C for 5 h in air to decompose the nitrate acid. To obtain fine particle, the calcined powder was manually ground for 1 h in ethanol and then dried. The ground powders of $Ni_{1-x}Co_xO$-YSZ were mixed with glycerol to form a slurry and then painted as the anode on one side of the YSZ electrolyte disk (15 mm diameter and 0.3 mm thick, Nikkato) with an area of 0.28 cm^2. After painting, the electrode was fired at 1300 °C for 3 h. The other side of the YSZ disk was paint with $La_{0.8}Sr_{0.2}MnO_3$-YSZ composite cathode slurry. The cathode slurry was prepared from the powder of 70%$La_{0.8}Sr_{0.2}MnO_3$ (LSM, Seimi Chemical) + 30%YSZ (wt.%) mixed with glycerol. The cathode was fired at 1200 °C for 3 h in air. The thickness of each electrode was approximately 70 μm. The platinum paste, which used as reference electrode, was pasted as a small circle closed to working anode with a small gap (2-3 mm) on the anode side. The 0.3 mm diameter of platinum mesh (#100 mesh) was used as a current lead. A Pyrex® glass ring was used to seal between the single cells and the alumina tube. The cells were fired at 850 °C for 30 min and the anode was then reduced at 800 °C for 2 h in a H_2 atmosphere prior to the measurement of the single cell performance at 750 °C under 20 v/v%CH_4 in He as fuel at a total flow rate of 20 cm^3/min. The cathode was fed with oxygen to use as an oxidant with the same rate as CH_4. The single cell performance was evaluated by the current-voltage (*I-V*) characterization. Impedance spectra were measured with a frequency response analyzer (FRA5097). After the single cell performance test, the operating temperature was maintained at 750 °C at a constant current, at 80 mA, to investigate the stability for 60 h by evaluating of impedance at 3, 6, 12, 24, 36, 48 and 60 h.

The $Ni_{1-x}Co_xO$-YSZ powders were also fired and reduced under the same condition as the anode to analyze the phase by x-ray diffraction (XRD). Morphology and carbon deposition were analysed by scanning electron microscopy (SEM) and energy-dispersive x-ray (EDX) analysis, respectively.

3 Results and discussion

3.1. Phase identification

Fig. 1 shows the XRD pattern of NiO-YSZ and $Ni_{0.85}Co_{0.15}O$-YSZ after reduction. The reduced NiO-YSZ composite (Fig. 1(a)) exhibited the diffraction pattern of face-centered cubic (fcc) Ni metal, according to ICDD 01-070-1849, and the diffraction pattern of YSZ, according to ICDD 01-070-4431, without impurities. The 111 and 200 diffraction peaks from the fcc Ni metal in the reduced $Ni_{0.85}Co_{0.15}O$-YSZ sample (Fig. 1(b)) ~~was~~ slightly shifted towards the direction of low 2θ values. This result indicated that NiO and $Ni_{0.85}Co_{0.15}O$ were completely reduced, and the Co was dissolved into the Ni phase and form a Ni–Co alloy. This result agreed to the binary Ni-Co phase diagram [23]. The shifts observed in the 111 and 200 peaks showed that the lattice constant of Ni was increased by Co alloying. The increase in the lattice parameters (*a*) was due to the ionic radius of Ni (0.69 Å), which is larger than that of Co (0.74 Å) [24].

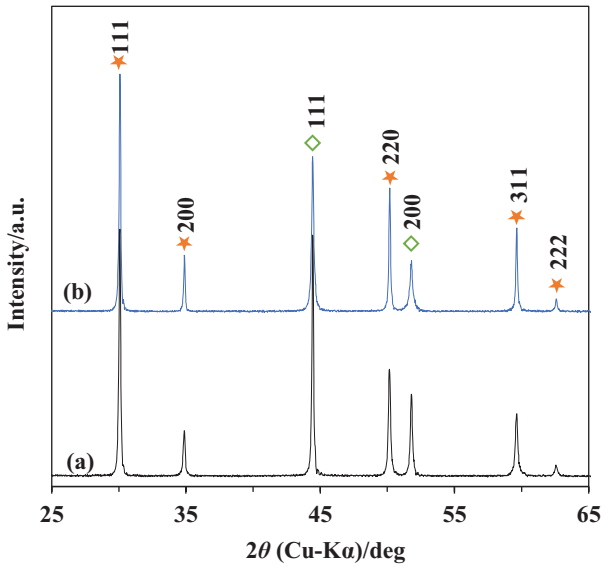

Figure 1. The XRD patterns of (a) NiO-YSZ and (b) $Ni_{0.85}Co_{0.15}O$-YSZ after reduction under an H_2 atmosphere at 800 °C for 2 h (★: $Ni_{1-x}Co_x$, ◇: YSZ)

3.2 Microstructure of anode

The cross-sectional microstructures of reduced $Ni_{1-x}Co_x$-YSZ cermet samples after sintering at 1300 °C for 3 h in air is shown in Fig. 2. Both anodes had a porous structure with well dispersed small metal particles. The $Ni_{0.85}Co_{0.15}$-YSZ showed a large grain size both in the metal alloy and YSZ compared to the Ni-YSZ. A coarsening of the YSZ particles was observed by Co alloying since Co_3O_4 can act as sintering aids [25].

3.3 Performance of SOFC

The *I-V* curves and power densities for Ni-YSZ and $Ni_{0.85}Co_{0.15}$-YSZ anodes at 750 °C in 20%v/vCH_4 in He are shown in Fig. 3. The $Ni_{0.85}Co_{0.15}$-YSZ anode showed a significantly higher performance than the Ni-YSZ. The maximum power densities of the single cells with the $Ni_{0.85}Co_{0.15}$-YSZ anode was 136 mW/cm^2, which was increased from 94 mW/cm^2 for the Ni-YSZ, approximately 44%.

The AC impedance spectra for the Ni-YSZ and $Ni_{0.85}Co_{0.15}$-YSZ anodes at 750 °C in CH_4 are compared in Fig. 4. The left intercept of the impedance spectra at high frequencies on the real axis (Re(*Z*)) indicated the ohmic resistance (R_o) which was mainly contributed by the ionic resistance of the electrolyte and electrodes-electrolyte connectivity, while the right intercept on the Re(*Z*) corresponded to the total resistance (R_{tot}). The subtraction of the ohmic resistance from the total resistance (R_{tot}-R_o) was the polarization resistance (R_p) which is mainly generated from a charge-transfer process

(corresponding to the electrode reaction) and a mass-

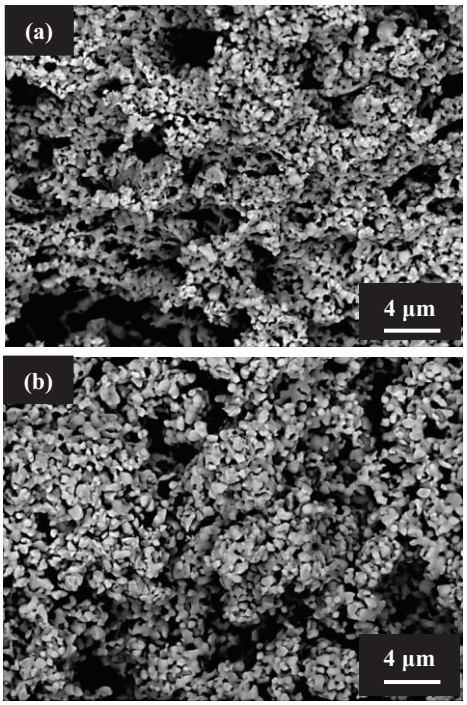

Figure 2. SEM images of (a) Ni-YSZ and (b) $Ni_{0.85}Co_{0.15}$-YSZ after reduction under an H_2 atmosphere at 800 °C.

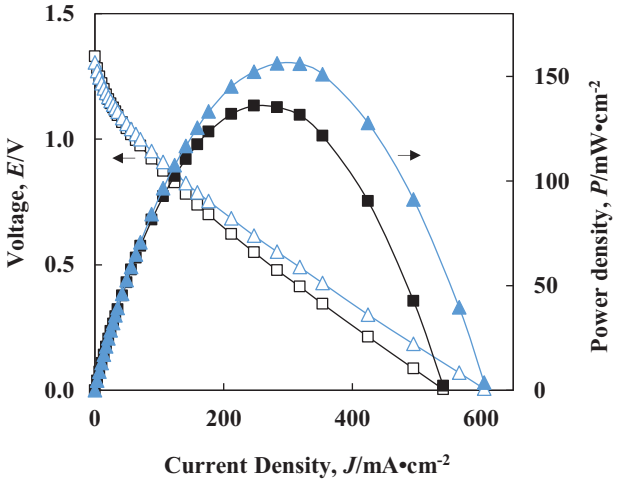

Figure 3. The current-voltage (*I-V*) curves (open symbols) and power densities (solid symbols) for (□,■) Ni-YSZ and (△,▲) $Ni_{0.85}Co_{0.15}$-YSZ anodes under an CH_4 atmosphere at 750 °C.

transfer process (corresponding to the gas diffusion, adsorption and dissociation on electrodes surface process) [26,27]. Since we used the same cathode and electrolyte, the difference in impedance arc was influenced by the anode resistance and its interface. The R_o and R_p decreased with the Co-alloying, as shown in Fig. 4, indicating that the alloying of Co in the Ni-YSZ can enhance the cell performance. The decrease in R_o by Co alloying is related to the microstructural change of the anode, as shown in Fig. 2. An improvement in the uniformity of grain connectivity most likely contributed to the decrease in the anode-electrolyte material resistance. R_p was also decreased by Co alloying, which was probably caused the formation of porous structure favorable for the diffusion of CH_4 molecules to the reaction site with the O^{2-} ions transported through the electrolyte. On the contrary, the Ni-YSZ showed the small grain size, which packed densely and provided a small porous structure resulting in a limited CH_4 diffusion.

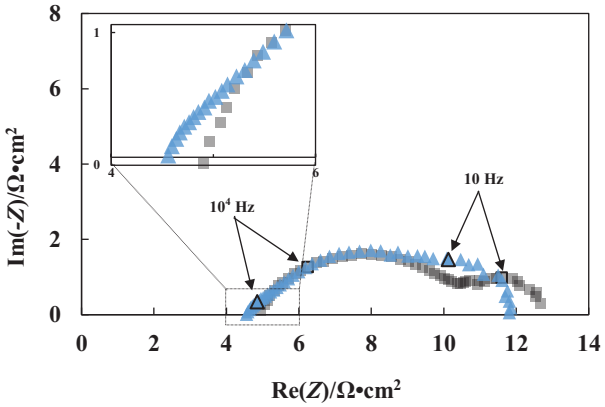

Figure 4. The impedance spectra for (■) Ni-YSZ and (▲) $Ni_{0.85}Co_{0.15}$-YSZ anodes under an CH_4 atmosphere at 750 °C.

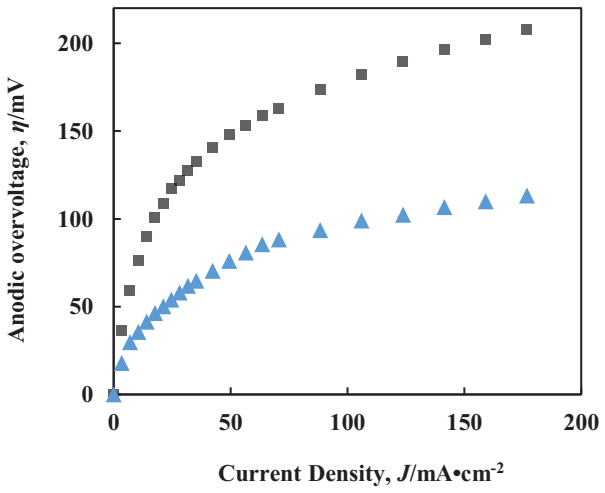

Figure 5. The anodic overvoltage for (■) Ni-YSZ and (▲) $Ni_{0.85}Co_{0.15}$-YSZ anodes under an CH_4 atmosphere at 750 °C.

Fig. 5 shows a comparison of the anodic overvoltage between the Ni-YSZ and $Ni_{0.85}Co_{0.15}$-YSZ. The anodic overvoltage for the $Ni_{0.85}Co_{0.15}$-YSZ was significantly lower than that for the Ni-YSZ, which corresponds to the behavior in the cell performance and R_p.

3.4 Stability of SOFC

To evaluate the long-term stability of the electrochemical performance, the impedance of the single cell for the Ni-YSZ and $Ni_{0.85}Co_{0.15}$-YSZ cells in the same CH_4 atmosphere were investigated at 750 °C for 60 h at a constant loaded current, 80 mA, for each cell. The ohmic resistance (R_o) and the polarization resistance (R_p) were

plotted as a function of time, as exhibited in Fig. 6. $Ni_{0.85}Co_{0.15}$-YSZ showed an almost constant R_o and a slight increase in R_p, while the Ni-YSZ showed increases in both R_o and R_p. This result was caused by the carbon deposition onto the anode surface of Ni-YSZ, which limited the gas diffusion to the anode surface. Moreover, the carbon deposition at the triple-phase boundary (TPB) of the anode, where electrochemical reaction takes place, resulted in a decrease in the length of TPB. The surface morphologies and carbon deposition on the Ni-YSZ and $Ni_{0.85}Co_{0.15}$-YSZ anode were verified by SEM and a qualitative EDX analysis, respectively. The surface morphologies of the Ni-YSZ and the $Ni_{0.85}Co_{0.15}$-YSZ are illustrated in Figs. 7(a) and (b), while the EDX spectra of each anode were showed in the inlet of each micrograph. A significant amount of carbon was detected on the Ni-YSZ anode, whereas a very small amount of carbon was observed on the $Ni_{0.85}Co_{0.15}$-YSZ. This result corresponds to the previous report [22] that the rate of carbon deposition was decreased dramatically by increasing Co content in the Ni-GDC. This process was the most similar as Sn surface alloying in Ni [28] which can suppress the C-C bond formation and/or reduce the thermodynamic driving force for carbon nucleation on low-coordinated sites [29].

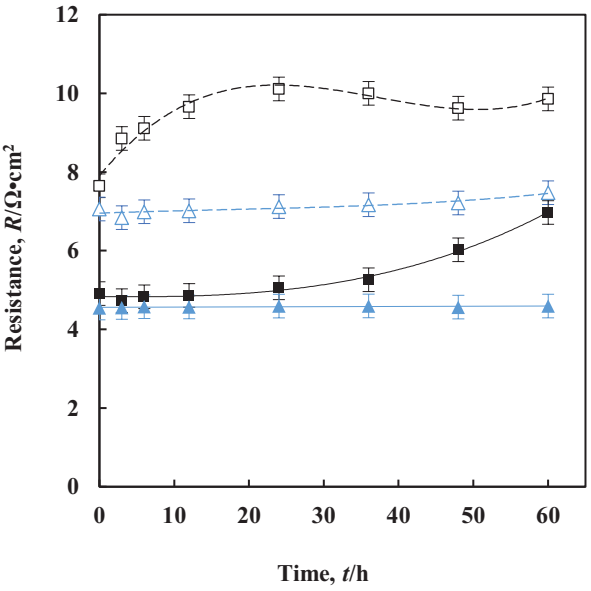

Figure 6. The ohmic resistance (solid symbols) and the polarization resistance (open symbols) as a function of time for (■,□) Ni-YSZ and (▲,△) $Ni_{0.85}Co_{0.15}$-YSZ anodes under a CH_4 atmosphere at 750 °C at a constant loaded current 80 mA.

4 Conclusion

The 15 mol% Co alloying in the Ni-YSZ anode has been investigated as an alternative SOFC anode material, which can be used for an operation by methane fuels. The introduced Co was completely alloyed in the Ni metal matrix phase. The alloying of Co in Ni affected the growth of Ni grains and reduced the electrical resistance and anodic overvoltage, which consequently improved the fuel cell performance of the Ni-YSZ cermet anode in CH_4 atmosphere. The doping of Co improved the stability of the electrochemical performance of the Ni-YSZ cermet anode in CH_4 fuel at 750 °C for 60 h, which was mainly caused by reducing the carbon deposition due to a suppression of the C-C bond formation and/or reducing the required thermodynamic driving force for the nucleation and growth of graphite.

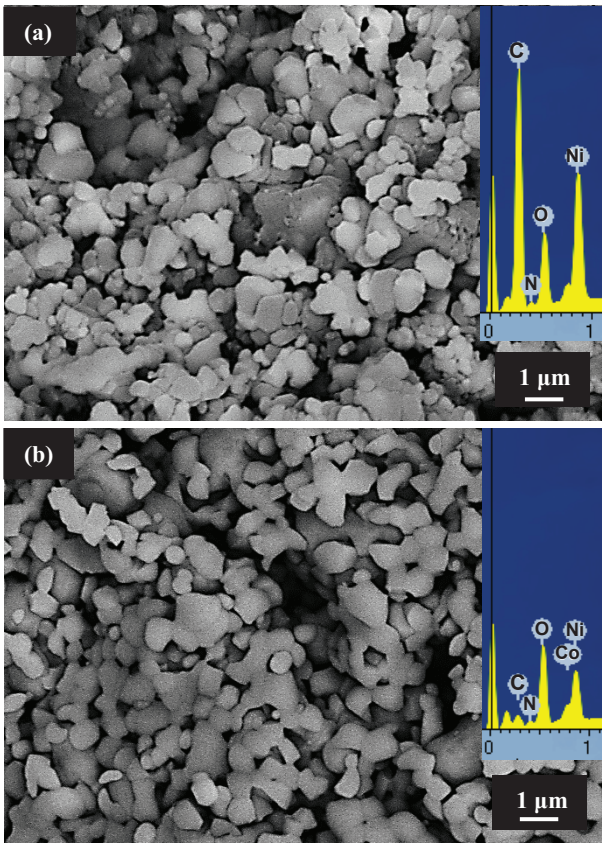

Figure 7. SEM surface micrographs and EDX spectra of Ni-YSZ and $Ni_{0.85}Co_{0.15}$-YSZ anodes after a stability test under an CH_4 atmosphere at 750 °C for 60 h.

References

1. A. Atkinson, S. Barnett, R. J. Gorte, J. T. S. Irvine, A. J. McEvoy, M. Mogensen, S. C. Singhal, J. Vohs, Nat. Mater., **3**, 17 (2004)
2. Z. Zhan, S. A. Barnett, Science, **308**, 844 (2005)
3. S. Park, J. M. Vohs, R. J. Gorte, Nature, **404**, 265 (2000)
4. J. Liu, S. A. Barnett, Solid State Ionics, **158**, 11 (2003).
5. E. N. Armstrong, J. Park, N. Q. Minh, Electrochem. Solid-State Lett., **15**, B75 (2012)
6. R. Muccillo, E. N. S. Muccillo, F. C. Fonseca, D. Z. de Florio, J. Electrochem. Soc., **155**, B232 (2008)
7. P. Kaparaju, I. Buendia, L. Ellegaard, I. Angelidakia, Bioresour. Technol., **99**, 4919 (2008)
8. C. H. Ting, D. J. Lee, Int. J. Hydrogen Energy, **32**, 677 (2007)
9. M. S. Fountoulakis, T. Manios, Bioresour. Technol., **100**, 3043 (2009)
10. N. Sanphoti, S. Towprayoon, P. Chaiprasert, A. Nopharatana, J. Environ. Manage., **81**, 27 (2006)
11. R. J. Gorte, J. M. Vohs, J. Catal., **216**, 477 (2003)

12. K. Sasaki, Y. Teraoka, J. Electrochem. Soc., **150**, A878 (2003)
13. D. Mogensen, J. D. Grunwaldt, P. V. Hendriksen, K. Dam-Johansen, J.U. Nielsen, J. Power Sources, **196(1)**, 25 (2010)
14. H. Kim, C. Lu, W. L. Worrell, J. M. Vohs, R. J. Gorte, J. Electrochem. Soc., **149**, A247 (2002)
15. A. Sin, E. Kopnin, Y. Dubitsky, A. Zaopo, A. S. Arico, D. L. Rosa, L. R. Gullo, V. Antonucci, J. Power Sources, **164**, 300 (2007)
16. A. Ringuedé, J.A. Labrincha, J.R. Frade, Solid State Ion., **141–142**, 549 (2001)
17. S. McIntosh, J. M. Vohs, R. J. Gorte, J. Electrochem. Soc., **150**, A470 (2003)
18. S. Jung, C. Lu, H. P. He, K. Ahn, R. J. Gorte, J. M. Vohs, J. Power Sources, **154**, 42 (2006)
19. N. Q. Minh, J. Am. Ceram. Soc., **76**, 563 (1993)
20. A. Ringuedé, D. Bronine, J.R. Frade, Electrochem. Acta, **48**, 437 (2002)
21. C.M. Grgicak, M.M. Pakulska, J. S. O'Brien, J. B. Giorgi, J. Power Sources, **183**, 26 (2008)
22. C.K. Cho, B.H. Choi, K.T. Lee, Journal of Alloys and Compounds, **541**, 433 (2012)
23. T. Nishizawa, T.B. Massalski (Ed.), *Binary Alloy Phase Diagrams,* **2**, 1214 (1990)
24. R. Shannon, Acta Crystallogr., 751 (1976)
25. G.C. Silva, E.N.S. Muccillo, Solid State Ion., **180**, 835 (2009)
26. M. Brown, S. Primdahl, M. Mogensen, J. Electrochem. Soc., **147**, 475 (2000).
27. H. Nakajima, T. Kitahara, T. Konomi, J. Electrochem. Soc., **157**, B1686 (2010)
28. E. Nikolla, J.W. Schwank, S. Linic, Catal. Today, **136**, 243 (2008)
29. E. Nikolla, J. W. Schwank, S. Linic, J. Catal., **250**, 85 (2007)